DMD Fast Forward. Published on January 19, 2007 as doi:10.1124/dmd.106.012294

Use of plasma and brain unbound fractions to assess the extent of brain distribution of thirty-four drugs: Comparison of unbound concentration ratios to *in vivo* P-glycoprotein efflux ratios

Authors:

J. Cory Kalvass, Tristan S. Maurer, and Gary M. Pollack

Institution:

School of Pharmacy, University of North Carolina, Chapel Hill, NC 27599-7360, USA (J.C.K, G.M.P)

Department of Pharmacokinetics, Dynamics and Metabolism, Pfizer Global Research and Development, Groton, CT 06340, USA (T.S.M.)

DMD Fast Forward. Published on January 19, 2007 as DOI: 10.1124/dmd.106.012294
This article has not been copyedited and formatted. The final version may differ from this version.

Running Title: Comparison of $[plasma]_{,u}/[brain]_{,u}$ and P-gp efflux ratios

Corresponding author: Gary M. Pollack, Ph.D.

Kerr Hall C.B.# 7360 University of North Carolina, Chapel Hill, NC 27599-7360

Phone: 919-962-0055

Fax: 919-966-0197

Email: gary_pollack@unc.edu

Text Status:
Number of text pages: 30
Number of tables: 3
Number of figures: 3
Number of references: 28
Number of words (Abstract): 249/250
Number of words (Introduction): 846/750
Number of words (Discussion): 1580/1500

Abbreviations used:

BBB, blood-brain barrier; CNS, central nervous system; CSF, cerebrospinal fluid; MS, mass spectrometry; HPLC, high-performance liquid chromatography; P-gp, P-glycoprotein

DMD Fast Forward. Published on January 19, 2007 as DOI: 10.1124/dmd.106.012294
This article has not been copyedited and formatted. The final version may differ from this version.

Abstract

The P-glycoprotein (P-gp)-deficient mouse model is used to assess the influence of P-gp-mediated efflux on the central nervous system (CNS) distribution of drugs. The steady-state unbound plasma-to-unbound brain concentration ratio ($[plasma]_{,u}/[brain]_{,u}$) is an alternative method for assessing CNS distribution of drugs independent of the mechanism(s) involved. The objective of this study was to compare the degree of CNS distributional impairment determined from the *in vivo* P-gp efflux ratio to that determined from the $[plasma]_{,u}/[brain]_{,u}$ ratio. CNS distribution of 34 drugs, including opioids, triptans, protease inhibitors, antihistamines, and other clinically-relevant drugs with either poor CNS distribution or blood-brain barrier (BBB) efflux, was studied. Plasma and brain unbound fractions were determined by equilibrium dialysis. $K_{p,brain}$ and the P-gp efflux ratio were obtained from the literature or determined experimentally. The P-gp efflux ratio and the $[plasma]_{,u}/[brain]_{,u}$ ratio were in concurrence (<3-fold difference) for 21 of the 34 drugs. However, the $[plasma]_{,u}/[brain]_{,u}$ ratio exceeded the P-gp efflux ratio substantially (>4-fold) for 10 of the 34 drugs, suggesting that other, non-P-gp-mediated mechanism(s) may limit the CNS distribution of these drugs. The P-gp efflux ratio exceeded the $[plasma]_{,u}/[brain]_{,u}$ ratio by more than 3-fold for 3 drugs, suggesting the presence of active uptake mechanism(s). These observations indicate that when mechanisms other than P-gp affect CNS distribution (non-P-gp-mediated efflux, poor passive permeability, cerebrospinal fluid (CSF) bulk flow, metabolism, or active uptake), the P-gp efflux ratio may under- or over-estimate CNS distributional impairment. The $[plasma]_{,u}/[brain]_{,u}$ ratio provides a simple mechanism-independent alternative for assessing the CNS distribution of drugs.

DMD Fast Forward. Published on January 19, 2007 as DOI: 10.1124/dmd.106.012294
This article has not been copyedited and formatted. The final version may differ from this version.

Introduction

The efflux transporter P-glycoprotein (P-gp) attenuates the CNS distribution of many drugs, including opioids, triptans, protease inhibitors, and antihistamines. One method used to assess the influence of P-gp on the CNS distribution of compounds is the P-gp-deficient mouse model. The P-gp efflux ratio, calculated from the ratio of brain-to-plasma partition coefficient ($K_{p,brain}$) in P-gp-deficient (*mdr1a*-/-) mice to $K_{p,brain}$ in P-gp-competent (*mdr1a*+/+) mice, reflects the degree to which P-gp-mediated efflux attenuates CNS distribution. However, when other processes influence CNS distribution, the P-gp efflux ratio may be a poor indicator of the degree to which CNS distribution of a compound is impaired.

$K_{p,brain}$ is the most widely used *in vivo* parameter for assessing the extent of CNS distribution. A common assumption is that compounds with large $K_{p,brain}$ values have more extensive CNS distribution than compounds with small $K_{p,brain}$ values. For example, a $K_{p,brain} \geq 1$ is often used as an arbitrary cutoff to classify compounds as having "good" CNS distribution, while a $K_{p,brain} << 1$ is used to classify compounds as having "poor" CNS distribution. While this type of classification is common, it may be misleading. It is recognized that tissue partition coefficients such as $K_{p,brain}$ are influenced by the relative binding affinity of a substrate for proteins in plasma versus the proteins in the tissue in question (Gillette, 1971; Kurz and Fichtl, 1983). For a compound that distributes solely by passive diffusion, at distribution equilibrium the unbound concentration in tissue will equal the unbound concentration in plasma, and the steady-state tissue partition coefficient is simply a function of the relative plasma and tissue unbound fractions (i.e., $K_{p,tissue} = f_{u,plasma} / f_{u,tissue}$). When brain and plasma unbound fractions are similar, than a $K_{p,brain} \sim 1$ would be consistent with unrestricted distribution solely by passive processes. However, the $K_{p,brain}$ value by itself provides little information without knowledge of brain and

DMD Fast Forward. Published on January 19, 2007 as DOI: 10.1124/dmd.106.012294
This article has not been copyedited and formatted. The final version may differ from this version.

plasma unbound fractions. A $K_{p,brain}$ value <1 could be the result of more extensive binding to plasma proteins than to proteins in brain tissue. Alternatively, a $K_{p,brain}$ value <1 it could reflect significant impairment in CNS distribution due to processes such as efflux transport at the blood-brain barrier (BBB).

Several recent literature reports have utilized the $f_{u,plasma}/f_{u,brain}$ ratio to predict $K_{p,brain}$ and to assess the CNS distribution of compounds. In one published account, the utility of the $f_{u,plasma}/f_{u,brain}$ ratio to predict the $K_{p,brain}$ of CNS discovery compounds was assessed (Kalvass and Maurer, 2002). As expected, the $f_{u,plasma}/f_{u,brain}$ ratio predicted the $K_{p,brain}$ for compounds that did not evidence active efflux at the BBB, and over-predicted $K_{p,brain}$ when active efflux at the BBB limited brain uptake. The degree to which the $f_{u,plasma}/f_{u,brain}$ ratio over-predicted $K_{p,brain}$ was identical to the P-gp efflux ratio for the single member of the compound set for which the P-gp efflux ratio had been determined. Another study used the $f_{u,plasma}/f_{u,brain}$ ratio to predict $K_{p,brain}$ and to assess the CNS distribution of 33 marketed CNS drugs (Maurer et al., 2004). The $f_{u,plasma}/f_{u,brain}$ ratio predicted the $K_{p,brain}$ value for the majority of CNS drugs (25 of 33), indicating that most CNS drugs do not have impaired CNS distribution. In those cases for which the $f_{u,plasma}/f_{u,brain}$ ratio did not predict $K_{p,brain}$, the discrepancy could be explained by active efflux or poor BBB permeability. More recently, for compounds subject to active efflux, the $f_{u,plasma}/f_{u,brain}$ ratio combined with *in vitro* efflux data was shown to provide superior estimates of $K_{p,brain}$ as compared to the $f_{u,plasma}/f_{u,brain}$ ratio alone (Summerfield et al., 2005).

When CNS distribution is impaired, the $f_{u,plasma}/f_{u,brain}$ ratio over-predicts $K_{p,brain}$. The magnitude of the over-prediction is reflective of the degree to which unbound plasma concentrations exceed unbound brain concentrations (eq. 1).

DMD Fast Forward. Published on January 19, 2007 as DOI: 10.1124/dmd.106.012294
This article has not been copyedited and formatted. The final version may differ from this version.

$$\text{Magnitude of over - prediction} = \frac{\left(\frac{f_{u,plasma}}{f_{u,brain}}\right)}{K_{p,brain}} = \frac{\left(\frac{f_{u,plasma}}{f_{u,brain}}\right)}{\frac{[brain]}{[plasma]}} = \frac{[plasma]_u}{[brain]_u} \qquad \text{(eq. 1)}$$

As shown in equation 1, the $f_{u,plasma}/f_{u,brain}$ ratio and $K_{p,brain}$ can be used to calculate the unbound plasma-to-unbound brain concentration ratio $[plasma]_{,u}/[brain]_{,u}$. The $[plasma]_{,u}/[brain]_{,u}$ ratio represents the degree to which unbound plasma concentrations exceed unbound brain concentrations and is meaningful expression of the degree of impairment in CNS distribution. A $[plasma]_{,u}/[brain]_{,u}$ ratio of unity for a given compound, is indicative of unimpaired CNS distribution (i.e., distribution consistent with passive diffusion; $[plasma]_u = [brain]_u$), while a $[plasma]_{,u}/[brain]_{,u}$ ratio greater than unity indicates impairment in CNS distribution (i.e., efflux uptake or poor BBB permeability; $[plasma]_u > [brain]_u$). In contrast, a $[plasma]_{,u}/[brain]_{,u}$ ratio values less than unity is consistent with enhanced CNS distribution (i.e., active uptake; $[plasma]_u < [brain]_u$).

The $[plasma]_{,u}/[brain]_{,u}$ ratio is expected to be equal to the *in vivo* P-gp efflux if P-gp-mediated efflux is the only active process affecting brain disposition. Using this principle, the present study was conducted to compare the degree of CNS distributional impairment expressed as the $[plasma]_{,u}/[brain]_{,u}$ ratio to the P-gp efflux ratio for 34 marketed drugs. Opioids, triptans, protease inhibitors, and antihistamines (n = 24 total) were included in this analysis because these classes of agents are known to include P-gp substrates, and the extent to which these compounds distribute into the CNS may have important implications regarding safety and efficacy. In addition, 10 marketed drugs from various drug classes with either poor CNS distribution or BBB efflux also were included as part of the analysis.

DMD Fast Forward. Published on January 19, 2007 as DOI: 10.1124/dmd.106.012294
This article has not been copyedited and formatted. The final version may differ from this version.

Material and Methods

Materials. Sufentanil was obtained from Abbott Laboratories (North Chicago, IL). Amprenavir, indinavir, nelfinavir, ritonavir, and saquinavir were obtained through the NIH AIDS Research and Reference Reagent Program, Division of AIDS, NIAID, NIH (Rockville, MD). Olanzapine was obtained from Pfizer Global Material Management (Groton, CT). Eletriptan was extracted from 40-mg tablets obtained from the Roerig Division of Pfizer (New York, NY), and the raw extract was used as a stock solution. Cetirizine, desloratadine, rizatriptan, and zolmitriptan were purchased from Sequoia Research (Oxford, UK). Alfentanil was obtained from Taylor Pharmaceuticals (Decatur, IL). Naratriptan and sumatriptan were purchased from U.S. Pharamcopoeia (Rockville, MD). All other drugs were purchased from Sigma-Aldrich (St. Louis, MO). Solvents and other reagents were obtained from common sources and were of reagent grade or better.

Drug Selection. Twenty-four marketed drugs from four main drug classes (7 opioids, 5 triptans, 5 protease inhibitors, and 7 antihistamines) were chosen for this study because drugs within each class exhibit varying degrees of interaction with BBB P-gp and because the extent of CNS distribution is known to be important to the efficacy and/or toxicity of these drug classes. In addition, 10 marketed drugs from other drug classes with either poor CNS distribution or BBB efflux also were chosen to assess the general utility of the approach with as diverse a dataset as possible.

Animals. Male CF-1 *mdr1a*(+/+) and *mdr1a*(-/-) mice (30-40 g; Charles River Laboratories, Inc., Wilmington, MA) were maintained on a 12-h light/dark cycle in a temperature- and humidity-controlled room with access to water and food ad libitum. All procedures involving

DMD Fast Forward. Published on January 19, 2007 as DOI: 10.1124/dmd.106.012294
This article has not been copyedited and formatted. The final version may differ from this version.

mice were approved by The Institutional Animal Care and Use Committee of the University of North Carolina and were conducted in accordance with "Principles of Laboratory Animal Care" (NIH Publication No. 85-23, revised in 1985).

Determination of $K_{p,brain}$ from animal studies. $K_{p,brain}$ values in *mdr1a*(-/-) and *mdr1a*(+/+) mice were obtained from the literature or, when published values were not available, were determined experimentally. Separate pharmacokinetic studies were conducted in *mdr1a*(-/-) and *mdr1a*(+/+) mice to determine the $K_{p,brain}$ values for alfentanil, fentanyl, loperamide, and methadone. Briefly, mice received a subcutaneous dose of the opioid, and at designated time points (9 time points, n=4 animals per time point) mice were sacrificed and trunk blood and brain tissue were collected. Plasma was harvested following centrifugation. Brain and plasma samples were stored at -20°C until analysis by HPLC-MS/MS (see below). $K_{p,brain}$ was determined from the ratio of brain to plasma $AUC_{0-\infty}$. $K_{p,brain}$ values for cimetidine, meperidine, ranitidine, and sufentanil were determined under steady-state conditions in *mdr1a*(-/-) and *mdr1a*(+/+) mice. Briefly, osmotic mini pumps (Alzet, Cupertino, CA) were implanted subcutaneously per the manufacture's instructions. Mice were sacrificed and trunk blood and brain tissue collected (n=3) 24 hr later. Plasma was harvested following centrifugation, and brain and plasma samples were stored at -20°C until analysis by HPLC-MS/MS (see below). $K_{p,brain}$ was calculated from the ratio of the 24-hr brain and plasma concentrations. All other $K_{p,brain}$ values were obtained from the literature.

Equilibrium dialysis experiments. Plasma and brain unbound fractions were determined in a 96-well equilibrium dialysis apparatus (HTDialysis, Gales Ferry, CT) using a previously reported method (Kalvass and Maurer, 2002). Briefly, fresh CF-1 or FVB mouse plasma and brain tissue were obtained the day of the study. Spectra-Por 2 membranes obtained from

DMD Fast Forward. Published on January 19, 2007 as DOI: 10.1124/dmd.106.012294
This article has not been copyedited and formatted. The final version may differ from this version.

Spectrum Laboratories Inc. (Rancho Dominguez, CA) were conditioned in HPLC-grade water for 15 min, followed by 30% ethanol for 15 min and 100 mM sodium phosphate buffer (pH 7.4) for 15 min. Brain tissue was diluted 3-fold with 100 mM sodium phosphate buffer (pH 7.4) and homogenized with a sonic probe. The drug of interest was added to plasma and brain homogenate to achieve a final concentration of 3 and 1 μM, respectively; 150-μl aliquots (n=6) were loaded into the 96-well equilibrium dialysis apparatus and dialyzed against and equal volume of 100 mM sodium phosphate (pH 7.4) buffer. The 96-well equilibrium dialysis apparatus was incubated for 4.5 hr in a 155 rpm shaking water bath maintained at 37˚C. Prior experience with the equilibrium dialysis apparatus indicated that equilibrium would be achieved by 4.5 hr (data not shown). After 4.5 hr, 10 μl of matrix sample (plasma or brain homogenate) and 50 μl of buffer sample were removed from the apparatus and added directly to HPLC vials containing 100 μl of methanol containing an appropriate internal standard. A 50-μl aliquot of control buffer was added to the brain homogenate and plasma samples, and either a 10-μl aliquot of control brain homogenate or control plasma was added to the buffer samples to yield identical sample composition between buffer and non-buffer samples. The samples were vortex-mixed, centrifuged, and the supernatant was analyzed by HPLC-MS/MS. Plasma unbound fraction was calculated from the ratio of concentrations determined from the plasma and buffer samples. Equation 2, a previously described approach to account for the effect of tissue dilution on unbound fraction (Kalvass and Maurer, 2002), was used to calculate the brain unbound fraction:

$$\text{Undiluted } f_u = \frac{1/D}{((1/f_{u,measured}) - 1) + 1/D} \qquad \text{(eq. 2) where}$$

D represents the fold dilution of brain tissue and $f_{u,measured}$ is the ratio of concentrations determined from the buffer and brain homogenate samples

DMD Fast Forward. Published on January 19, 2007 as DOI: 10.1124/dmd.106.012294
This article has not been copyedited and formatted. The final version may differ from this version.

HPLC-MS/MS Analysis of samples. All samples were quantified using either a PE-Sciex API-3000 (Turbo Ionspray source, 500˚C) or an API-4000 (Turbo V Ionspray source, 700˚C, PerkinElmerSciex Instruments, Boston, MA) quadruple mass spectrometer as summarized in Table 1. Equilibrium dialysis samples were prepared as described in the equilibrium dialysis section. Plasma and brain samples from animal experiments were prepared as follows. Brain samples were homogenized in water (1:2 v/v) with a sonic probe. An aliquot of homogenate or serum (2 to 25 µl) was transferred to a HPLC vial, and protein was precipitated with 4- to 125-volumes of methanol containing an appropriate internal standard. The sample was vortex-mixed, centrifuged, and the supernatant was analyzed by HPLC-MS/MS. Samples were injected (2-10 µl; CTC Analytics autosampler, Zwingen, Switzerland) onto either a Phenomenex 2.0 × 30 mm, 5 µm Gemini 110A or a Phenomenex 2.0 × 30 mm, 4 µm Synergi Max-RP column (Phenomenex, Torrance, CA) maintained at room temperature. The total run time was 3 min. Analytes were eluted with a linear gradient consisting of ammonium acetate (pH 6.8; 10 mM) ["A"], methanol ["B"] and acetonitrile ["C"] produced by three Shimadzu LC-10ADVP binary pumps. An initial condition (80-95% "A") was ramped to an intermediate condition (5-25% "A") over 2 min, held for 0.5 min at the intermediate condition, and then returned initial conditions in a single step to re-equilibrate the column (Table 1). During the run, the flow rate was increased from 750 to 1500 µl/min over the first 2 min, held at 1500 µl/min for 1 min, and then returned to the initial flow rate of 750 µl/min in a single step. For samples run on the API3000, the flow rate was increased from 500 to750 µl/min over the first 2 min, held at 750 µl/min for 1 min, and then returned to the initial flow rate of 500 µl/min in a single step. The entire column effluent was diverted from the source of the quadrupole mass spectrometer for the first 0.8 min and final 0.5 min of the run. Standards were prepared with either plasma or brain

DMD Fast Forward. Published on January 19, 2007 as DOI: 10.1124/dmd.106.012294
This article has not been copyedited and formatted. The final version may differ from this version.

homogenate and were identical in final composition to corresponding samples. Accuracy of standards was within ± 20%.

Data analysis. The *in vivo* P-gp efflux ratio for each drug was calculated as the ratio of *mdr1a*(-/-) and *mdr1a*(+/+) $K_{p,brain}$ values. The steady-state $[plasma]_{,u}/[brain]_{,u}$ ratio was calculated for each drug according to equation 3, where $K_{p,brain}$ is the value from P-gp competent mice.

$$\frac{[plasma]_u}{[brain]_u} = \frac{1}{K_{p,brain,}} \times \frac{f_{u,plasma}}{f_{u,brain}} \qquad \text{(eq. 3)}$$

The P-gp efflux ratio and $[plasma]_{,u}/[brain]_{,u}$ ratio were used to assess the distributional behavior of each drug based on the graphical scheme in Figure 1. The horizontal and vertical lines represent the point at which the P-gp efflux ratio and the $[plasma]_{,u}/[brain]_{,u}$ ratio equal 3, respectively. A P-gp efflux ratio or $[plasma]_{,u}/[brain]_{,u}$ ratio >3 was considered meaningful because such ratio is sufficiently different than unity and that most CNS drugs (29 out of 32) have been shown to have P-gp efflux ratios <3 (Doran et al., 2005). The figure was divided into four quadrants (I-IV) based on whether the P-gp efflux or $[plasma]_{,u}/[brain]_{,u}$ ratio values were greater than or less than 3. The solid line passing through the origin represents the line of identity ± 3-fold (dashed lines). Drugs were assessed as follows: quadrant I- impaired CNS distribution due to P-gp-mediated efflux; subsections Ia and Ib- impaired CNS distribution due to P-gp with other active process(es) present; quadrant II- impaired CNS distribution due to non-P-gp mechanism; quadrant III- no impairment in CNS distribution; quadrant IV- P-gp substrate, but CNS distribution is not impaired due to the presence of a compensatory mechanism. The CNS distribution behavior of the protease inhibitors, opioids, antihistamines, and triptans were evaluated separately.

DMD Fast Forward. Published on January 19, 2007 as DOI: 10.1124/dmd.106.012294
This article has not been copyedited and formatted. The final version may differ from this version.

Results

The $K_{p,brain}$, $f_{u,plasma}$, and $f_{u,brain}$ values for all drugs included in this study are reported in Table 2. The $K_{p,brain}$ and $f_{u,brain}$ values varied by more than 4 orders of magnitude, whereas the $f_{u,plasma}$ values varied by more than 3 orders of magnitude, among the drugs studied. Vinblastine was unstable in mouse plasma, so the $f_{u,plasma}$ value was reported as equal to or greater than the $f_{u,plasma}$ value determined from the buffer concentrations, assuming complete mass balance.

The P-gp efflux ratio and the $[plasma]_{,u}/[brain]_{,u}$ ratio were compared within each drug class (opioid, antihistamine, triptan, and protease inhibitor; Figure 2 A, B, C, and D, respectively). The P-gp efflux ratio and the $[plasma]_{,u}/[brain]_{,u}$ ratio for all 34 drugs examined in this study are compared in Figure 3.

The P-gp efflux ratios varied between ~1 and 50 for the examined drugs; 18 of the 34 drugs had a P-gp efflux ratio exceeding 3. The $[plasma]_{,u}/[brain]_{,u}$ ratio varied between ~1 and >1000, with 23 of the 34 drugs having a $[plasma]_{,u}/[brain]_{,u}$ ratio greater than 3. The P-gp efflux ratio and the $[plasma]_{,u}/[brain]_{,u}$ ratio were in concurrence (<3-fold difference) for 21 of the 34 drugs (quadrants I and III). However, the $[plasma]_{,u}/[brain]_{,u}$ ratio exceeded the P-gp efflux ratio substantially (>4-fold) for cetirizine, cimetidine, dexamethasone, digoxin, doxorubicin, fexofenadine, ivermectin, ranitidine, sumatriptan and zolmitriptan (quadrants Ib and II). The P-gp efflux ratio was more than 3-fold higher than the $[plasma]_{,u}/[brain]_{,u}$ ratio for methadone, ritonavir, and saquinavir (quadrant IV).

Discussion

The P-gp efflux ratio and the $[plasma]_{,u}/[brain]_{,u}$ ratio were in concurrence (<3-fold difference) for 21 of the 34 drugs studied. This concurrence indicates, that for most of the drugs examined, there was little difference between the P-gp efflux ratio and the $[plasma]_{,u}/[brain]_{,u}$ ratio, and that any impairment in CNS disposition would be consistent with P-gp-mediated efflux. The $[plasma]_{,u}/[brain]_{,u}$ ratio exceeded the P-gp efflux ratio substantially (>4-fold) for 10 of the 34 drugs studied (cetirizine, cimetidine, dexamethasone, digoxin, doxorubicin, fexofenadine, ivermectin, ranitidine, sumatriptan, and zolmitriptan), suggesting that other non-P-gp-mediated mechanism(s) may limit the CNS distribution of these drugs. The P-gp efflux ratio exceeded the $[plasma]_{,u}/[brain]_{,u}$ ratio by more than 3-fold for three of the drugs examined (methadone, ritonavir, and saquinavir), suggesting the presence of active uptake mechanism(s). The results for the opioids, triptans, protease inhibitors, and antihistamines are discussed separately in the following paragraphs.

Opioids. Consistent with their clinical use as analgesics, there was minimal impairment in CNS distribution (<3-fold as assessed by both the P-gp efflux ratio and the $[plasma]_{,u}/[brain]_{,u}$ ratio) for, sufentanil, fentanyl, morphine, and meperidine. Alfentanil evidenced modest impairment (~3-fold), consistent with P-gp-mediated efflux. Both methadone and loperamide were significant P-gp substrates (P-gp efflux ratios of 7 and 33, respectively). However, only loperamide had substantial impairment in CNS distribution as assessed by the $[plasma]_{,u}/[brain]_{,u}$ ratio.

The discrepancy between the P-gp efflux ratio and the $[plasma]_{,u}/[brain]_{,u}$ ratio for methadone may indicate the presence of one or more compensatory mechanism(s) (e.g., active uptake) that may have negated the impact of P-gp-mediated efflux. Methadone is a substrate for active

DMD Fast Forward. Published on January 19, 2007 as DOI: 10.1124/dmd.106.012294
This article has not been copyedited and formatted. The final version may differ from this version.

uptake in the lung (Chi and Dixit, 1977), so it is plausible methadone also may undergo active uptake across the BBB. The $[plasma]_{,u}/[brain]_{,u}$ ratio predicted that loperamide alone would have substantially reduced central activity, whereas the P-gp efflux ratio predicted that both loperamide and methadone would evidence substantially reduced central activity. Clinically, only loperamide is associated with reduced central activity, so the $[plasma]_{,u}/[brain]_{,u}$ ratio was better able to differentiate between opioids with and without reduced central activity than the P-gp efflux ratio.

Triptans. The $[plasma]_{,u}/[brain]_{,u}$ ratio indicated that all triptans examined have impaired CNS distribution. However, only rizatriptan and eletriptan showed significant impairment due to P-gp (>3-fold). Non-P-gp-mediated mechanism(s) may be responsible for impaired CNS distribution of sumatriptan and zolmitriptan (quadrant II). One non-P-gp-mediated mechanism that may impair the CNS distribution of sumatriptan and zolmitriptan is CSF bulk flow. When passive permeability and brain uptake clearance are very low, CSF bulk flow may represent a significant clearing mechanism from the CNS, ultimately resulting in reduced CNS exposure (Shen et al., 2004). Because sumatriptan and zolmitriptan both have very low passive permeability [less than the paracellular marker mannitol; (Mahar Doan et al., 2002)], it is plausible that CSF bulk flow may limit sumatriptan and zolmitriptan CNS distribution.

If triptans possess a degree of CNS distributional impairment in humans similar to that indicated by the $[plasma]_{,u}/[brain]_{,u}$ ratio, the impaired distribution may have important implications regarding mechanism of action and CNS side-effect profile of triptans. There is debate as to whether the anti-migraine action of triptans is solely through vascular-mediated events, or whether antinociceptive activity within the brain stem trigeminal nuclei is partially responsible (Dodick and Martin, 2004). In addition, the incidence of CNS side-effects varies

DMD Fast Forward. Published on January 19, 2007 as DOI: 10.1124/dmd.106.012294
This article has not been copyedited and formatted. The final version may differ from this version.

between the different triptans. By understanding the inter-relationships between *in vivo* efficacy, incidence of CNS side-effects, and the extent of CNS distribution, the optimal CNS distributional characteristics of triptans may be deduced.

Protease Inhibitors. All of the protease inhibitors examined undergo significant P-gp efflux (P-gp efflux ratio ≥ 7, quadrant I and IV). However, the $[plasma]_{,u}/[brain]_{,u}$ ratio indicated that ritonavir and saquinavir, despite being P-gp substrates, do not have impaired CNS distribution (< 3-fold). This observation may be explained if a compensatory mechanism (i.e., active uptake) negates the impact of P-gp-mediated efflux. This explanation is supported by reports demonstrating that both ritonavir and saquinavir are substrates for uptake transporters (Anthonypillai et al., 2004; Su et al., 2004).

Even though it has been thought that ritonavir and saquinavir have poor CNS distribution because of significant P-gp-mediated efflux (in vivo P-gp efflux ratio > 5) and low $K_{p,brain}$ (0.17 and 0.13, respectively), this may not necessarily be the case. The $[plasma]_{,u}/[brain]_{,u}$ ratio indicates that steady-state unbound concentrations in plasma and brain are approximately equal for these agents. Compensatory uptake mechanism(s) may overcome the efflux by P-gp, and the low $K_{p,brain}$ values therefore would simply be a function of more extensive protein binding in plasma than in brain. The binding of ritonavir and saquinavir to plasma proteins is higher than that in the brain. Therefore, based on $f_{u,plasma}$ and $f_{u,brain}$, the $K_{p,brain}$ is expected to be 0.25 and 0.22, respectively, and the $[plasma]_{,u}/[brain]_{,u}$ ratio indicates the BBB has no net effect on the CNS distribution of ritonavir and saquinavir. These observations suggest that compounds that evidence P-gp-mediated efflux together with low $K_{p,brain}$ ($K_{p,brain} << 1$) may not have impaired CNS distribution if active uptake counters the effects of P-gp efflux and if the low $K_{p,brain}$ can be explained by binding in plasma that exceeds binding in brain. Overall, ritonavir and saquinavir

DMD Fast Forward. Published on January 19, 2007 as DOI: 10.1124/dmd.106.012294
This article has not been copyedited and formatted. The final version may differ from this version.

may have better CNS distribution, and thus may be more effective in combating HIV viral infection in the CNS, than previously thought.

Antihistamines. Consistent with their central activity, the sedating antihistamines triprolidine, diphenhydramine, and hydroxyzine had minimal impairment in CNS distribution (quadrant III). The non-sedating histamines desloratadine and cetirizine fell within quadrants I and Ib, respectively, indicating substantial impairment in CNS distribution due to P-gp-mediated efflux. However, the P-gp efflux ratio did not indicate impairment in CNS distribution of the non-sedating antihistamine fexofenadine, whereas the $[plasma]_{,u}/[brain]_{,u}$ ratio suggested significant impairment (quadrant II). Non-P-gp-mediated mechanism(s) may contribute to the impairment in CNS distribution of cetirizine and fexofenadine (quadrants Ib and II). Assuming that loratadine is a pro-drug of desloratadine, only the $[plasma]_{,u}/[brain]_{,u}$ ratio correctly distinguished between the sedating and non-sedating antihistamines.

Other drugs with poor CNS distribution or BBB efflux. Other marketed drugs with poor CNS distribution or BBB efflux were examined along with the opioids, triptans, protease inhibitors, and antihistamines (Figure 3). As expected, P-gp substrates such as quinidine, verapamil, and paclitaxel fell within quadrant I (consistent with P-gp being the only efflux mechanism), while efflux substrates for transporters other than P-gp such as ranitidine, digoxin, and doxorubicin fell within quadrants Ib and II (Figure 3 and Table 3).

Discrepancy between P-gp efflux ratio and the $[plasma]_{,u}/[brain]_{,u}$ ratio. The P-gp efflux ratio and the $[plasma]_{,u}/[brain]_{,u}$ ratio differed by more than 3-fold for 13 of the 34 drugs examined. In most cases, the difference can be explained by the physiochemical properties, and/or transport characteristics of the individual drugs (Table 3). Ten of the 13 drugs for which discrepancy was noted were located in either quadrant Ib or II, indicating more extensive

DMD Fast Forward. Published on January 19, 2007 as DOI: 10.1124/dmd.106.012294
This article has not been copyedited and formatted. The final version may differ from this version.

impairment in CNS distribution than predicted by the P-gp efflux ratio. For these 10 drugs, six drugs (digoxin, doxorubicin, ivermectin, cimetidine, dexamethasone, and ranitidine) are known to be substrates for efflux transporters other than P-gp (Table 3), two (sumatriptan and zolmitriptan) have very low permeability values (less than mannitol), and two (cetirizine and fexofenadine) have reduced central activity relative to other drugs in the same class. The remaining three of the 13 drugs (methadone, ritonavir, and saquinavir) for which the P-gp efflux ratio and the $[plasma]_{,u}/[brain]_{,u}$ ratio differed by more than 3-fold were classified in quadrant IV, indicating less impairment in CNS distribution than indicated by the P-gp efflux ratio. One possible explanation for such drugs is the presence of a compensatory active uptake mechanism. Consistent with this explanation, all three of these drugs are substrates of active uptake (Table 3). Although not the intent of this work, additional detailed studies on individual drugs would be useful to confirm whether the discrepancy between the P-gp efflux ratio and the $[plasma]_{,u}/[brain]_{,u}$ ratio are real and are not experimental artifacts. For future studies examining the influence of non-P-gp-mediated mechanisms on CNS distribution, the 13 drugs identified as having discrepancies between the P-gp efflux ratio and the $[plasma]_{,u}/[brain]_{,u}$ ratio would be logical choices.

Accurate determination of steady-state $K_{p,brain}$ is necessary for accurate determination of the P-gp efflux ratio and the $[plasma]_{,u}/[brain]_{,u}$ ratio. In addition, accurate experimental determination of $f_{u,plasma}$ and $f_{u,brain}$ is required for accurate assessment of the $[plasma]_{,u}/[brain]_{,u}$ ratio. Any error in determining $K_{p,brain}$, $f_{u,plasma}$, or $f_{u,brain}$ may lead to artificial discrepancies between the P-gp efflux ratio and the $[plasma]_{,u}/[brain]_{,u}$ ratio which may also lead to incorrect conclusions regarding the CNS distribution of a compound. The likelihood this occurring can be

DMD Fast Forward. Published on January 19, 2007 as DOI: 10.1124/dmd.106.012294
This article has not been copyedited and formatted. The final version may differ from this version.

minimized by examining $K_{p,brain}$ over multiple time points to ensure steady-state $K_{p,brain}$ has been achieved and by using a validated method for determining $f_{u,plasma}$, and $f_{u,brain}$.

In summary the P-gp efflux ratio and $[plasma]_{,u}/[brain]_{,u}$ ratio were similar for most of the drugs examined, indicating P-gp-mediated efflux is the predominate mechanism limiting the CNS distribution of drugs in the selected compound set. The $[plasma]_{,u}/[brain]_{,u}$ ratio differentiated between sedating and non-sedating antihistamines and between opioids with and without reduced central activity, whereas the P-gp efflux ratio did not. Furthermore, when there were differences between the P-gp efflux ratio and the $[plasma]_{,u}/[brain]_{,u}$ ratio, additional supporting evidence was consistent with the $[plasma]_{,u}/[brain]_{,u}$ ratio. When mechanisms other than P-gp affect CNS distribution (non-P-gp-mediated efflux, poor passive permeability, CSF bulk flow, metabolism, or active uptake), the P-gp efflux ratio may under- or over-estimate CNS distributional impairment. The $[plasma]_{,u}/[brain]_{,u}$ ratio provides a simple alternative means for assessing the CNS distribution of drugs independent of the mechanism(s) involved.

References

Anthonypillai C, Sanderson RN, Gibbs JE and Thomas SA (2004) The distribution of the HIV protease inhibitor, ritonavir, to the brain, cerebrospinal fluid, and choroid plexuses of the guinea pig. *J Pharmacol Exp Ther* **308:**912-920.

Bourdet DL, Pritchard JB and Thakker DR (2005) Differential substrate and inhibitory activities of ranitidine and famotidine toward human organic cation transporter 1 (hOCT1; SLC22A1), hOCT2 (SLC22A2), and hOCT3 (SLC22A3). *J Pharmacol Exp Ther* **315:**1288-1297.

Chen C, Hanson E, Watson JW and Lee JS (2003) P-glycoprotein limits the brain penetration of nonsedating but not sedating H1-antagonists. *Drug Metab Dispos* **31:**312-318.

Chi CH and Dixit BN (1977) Characterization of (+/-)-methadone uptake by rat lung. *Br J Pharmacol* **59:**539-549.

Cvetkovic M, Leake B, Fromm MF, Wilkinson GR and Kim RB (1999) OATP and P-glycoprotein transporters mediate the cellular uptake and excretion of fexofenadine. *Drug Metab Dispos* **27:**866-871.

Dodick DW and Martin V (2004) Triptans and CNS side-effects: pharmacokinetic and metabolic mechanisms. *Cephalalgia* **24:**417-424.

Doran A, Obach RS, Smith BJ, Hosea NA, Becker S, Callegari E, Chen C, Chen X, Choo E, Cianfrogna J, Cox LM, Gibbs JP, Gibbs MA, Hatch H, Hop CE, Kasman IN, Laperle J, Liu J, Liu X, Logman M, Maclin D, Nedza FM, Nelson F, Olson E, Rahematpura S, Raunig D, Rogers S, Schmidt K, Spracklin DK, Szewc M, Troutman M, Tseng E, Tu M, Van Deusen JW, Venkatakrishnan K, Walens G, Wang EQ, Wong D, Yasgar AS and Zhang C (2005) The impact of P-glycoprotein on the disposition of drugs targeted for indications of the central nervous system: evaluation using the MDR1A/1B knockout mouse model. *Drug Metab Dispos* **33:**165-174.

Evans DC, O'Connor D, Lake BG, Evers R, Allen C and Hargreaves R (2003) Eletriptan metabolism by human hepatic CYP450 enzymes and transport by human P-glycoprotein. *Drug Metab Dispos* **31:**861-869.

Gillette JR (1971) Factors affecting drug metabolism. *Ann NY Acad Sci* **179**.

Hendrikse NH, Schinkel AH, de Vries EG, Fluks E, Van der Graaf WT, Willemsen AT, Vaalburg W and Franssen EJ (1998) Complete in vivo reversal of P-glycoprotein pump function in the blood-brain barrier visualized with positron emission tomography. *Br J Pharmacol* **124:**1413-1418.

Hindmarch I, Shamsi Z and Kimber S (2002) An evaluation of the effects of high-dose fexofenadine on the central nervous system: a double-blind, placebo-controlled study in healthy volunteers. *Clin Exp Allergy* **32:**133-139.

Kalvass JC and Maurer TS (2002) Influence of nonspecific brain and plasma binding on CNS exposure: implications for rational drug discovery. *Biopharm Drug Dispos* **23:**327-338.

Kemper EM, Cleypool C, Boogerd W, Beijnen JH and van Tellingen O (2004) The influence of the P-glycoprotein inhibitor zosuquidar trihydrochloride (LY335979) on the brain penetration of paclitaxel in mice. *Cancer Chemother Pharmacol* **53:**173-178.

Kim RB, Fromm MF, Wandel C, Leake B, Wood AJ, Roden DM and Wilkinson GR (1998) The drug transporter P-glycoprotein limits oral absorption and brain entry of HIV-1 protease inhibitors. *J Clin Invest* **101:**289-294.

Kurz H and Fichtl B (1983) Binding of drugs to tissues. *Drug Metab Rev* **14:**467-510.

Kusuhara H and Sugiyama Y (2001) Efflux transport systems for drugs at the blood-brain barrier and blood-cerebrospinal fluid barrier (Part 2). *Drug Discov Today* **6:**206-212.

Kusuhara H, Suzuki H, Terasaki T, Kakee A, Lemaire M and Sugiyama Y (1997) P-Glycoprotein mediates the efflux of quinidine across the blood-brain barrier. *J Pharmacol Exp Ther* **283:**574-580.

Lespine A, Dupuy J, Orlowski S, Nagy T, Glavinas H, Krajcsi P and Alvinerie M (2005) Interaction of ivermectin with multidrug resistance proteins (MRP1, 2 and 3). *Chem Biol Interact*.

Mahar Doan KM, Humphreys JE, Webster LO, Wring SA, Shampine LJ, Serabjit-Singh CJ, Adkison KK and Polli JW (2002) Passive permeability and P-glycoprotein-mediated efflux differentiate central nervous system (CNS) and non-CNS marketed drugs. *J Pharmacol Exp Ther* **303:**1029-1037.

Maurer TS, Debartolo DB, Tess DA and Scott DO (2004) Relationship between Exposure and Nonspecific Binding of Thirty-Three Central Nervous System Drugs in Mice. *Drug Metab Dispos*.

Pariante CM, Makoff A, Lovestone S, Feroli S, Heyden A, Miller AH and Kerwin RW (2001) Antidepressants enhance glucocorticoid receptor function in vitro by modulating the membrane steroid transporters. *Br J Pharmacol* **134:**1335-1343.

Polli JW, Jarrett JL, Studenberg SD, Humphreys JE, Dennis SW, Brouwer KR and Woolley JL (1999) Role of P-glycoprotein on the CNS disposition of amprenavir (141W94), an HIV protease inhibitor. *Pharm Res* **16:**1206-1212.

Schinkel AH, Mol CA, Wagenaar E, van Deemter L, Smit JJ and Borst P (1995a) Multidrug resistance and the role of P-glycoprotein knockout mice. *Eur J Cancer* **31A:**1295-1298.

Schinkel AH, Smit JJ, van Tellingen O, Beijnen JH, Wagenaar E, van Deemter L, Mol CA, van der Valk MA, Robanus-Maandag EC, te Riele HP and et al. (1994) Disruption of the mouse mdr1a P-glycoprotein gene leads to a deficiency in the blood-brain barrier and to increased sensitivity to drugs. *Cell* **77:**491-502.

Schinkel AH, Wagenaar E, van Deemter L, Mol CA and Borst P (1995b) Absence of the mdr1a P-Glycoprotein in mice affects tissue distribution and pharmacokinetics of dexamethasone, digoxin, and cyclosporin A. *J Clin Invest* **96:**1698-1705.

Shen DD, Artru AA and Adkison KK (2004) Principles and applicability of CSF sampling for the assessment of CNS drug delivery and pharmacodynamics. *Adv Drug Deliv Rev* **56:**1825-1857.

Su Y, Zhang X and Sinko PJ (2004) Human organic anion-transporting polypeptide OATP-A (SLC21A3) acts in concert with P-glycoprotein and multidrug resistance protein 2 in the vectorial transport of Saquinavir in Hep G2 cells. *Mol Pharm* **1:**49-56.

Summerfield S, Stevens AJ, Cutler L, Del Carmen Osuna M, Hammond B, Tang SP, Hersey A, Spalding DJ and Jeffrey P (2005) Improving the In Vitro Prediction of In Vivo CNS Penetration: Integrating Permeability, Pgp Efflux and Free Fractions in Blood and Brain. *J Pharmacol Exp Ther*.

Yamazaki M, Neway WE, Ohe T, Chen I, Rowe JF, Hochman JH, Chiba M and Lin JH (2001) In vitro substrate identification studies for p-glycoprotein-mediated transport: species difference and predictability of in vivo results. *J Pharmacol Exp Ther* **296:**723-735.

Footnotes

This work was supported by grant R01 GM61191 from the National Institutes of Health and Pfizer Inc. J. Cory Kalvass was supported by an Eli Lilly and Company Foundation Predoctoral Fellowship in Pharmacokinetics and Drug Disposition.

Legends to Figures

Figure 1. The CNS distributional behavior of each drug based on the plot scheme above. The horizontal and vertical lines represent the point at which the P-gp efflux ratio and the [plasma]-$_{,u}$/[brain]$_{,u}$ ratio equal 3, respectively. 3-fold impairment in CNS distribution was considered meaningful. The figure was divided in to four quadrants (I-IV) based on whether the P-gp efflux or ([plasma]$_{,u}$/[brain]$_{,u}$) ratio values were greater than or less than 3. The solid line passing through the origin represents the line of unity ± 3-fold (dashed lines). Drugs were assessed as follows: (quadrant I) impaired CNS distribution due to P-gp-mediated efflux, (subsections Ia and Ib) impaired CNS distribution due to P-gp with other active process(es) present; (quadrant II) impaired CNS distribution due to non-P-gp mechanism; (quadrant III) no impairment in CNS distribution; (quadrant IV) P-gp substrate, but CNS distribution is not impaired due to compensatory mechanism.

Figure 2. Comparison of the P-gp efflux ratio and the [plasma]$_{,u}$/[brain]$_{,u}$ ratio of (A) opioids, (B) triptans, (C) protease inhibitors and (D) antihistamines. The CNS distributional behavior of each drug was assessed according to the scheme in Figure 1. Symbols for drugs are defined in Table 2.

Figure 3. Comparison of the P-gp efflux ratio and the [plasma]$_{,u}$/[brain]$_{,u}$ ratio of all 34 marketed drugs. The CNS distributional behavior of each drug was assessed according to the scheme in Figure 1. As expected, P-gp substrates such as quinidine, verapamil, and paclitaxel fell within quadrant I (consistent with P-gp being the only efflux mechanism), while drugs subject to transport by other transporters or with poor BBB permeability, such as ranitidine, digoxin, and doxorubicin fell within quadrants Ib, II, or IV. Symbols for drugs are defined in Table 2.

Table 1. Conditions used for HPLC-MS/MS analysis for each drug. Column consisted of either a Phenomenex 2.0 × 30 mm, 5 µm Gemini 110A (column 1) or a Phenomenex 2.0 × 30 mm, 4 µm Synergi Max-RP column (column 2). Mobile phase A, B, C consisted of ammonium acetate (pH 6.8; 10 mM), methanol and acetonitrile, respectively. HPLC gradients with the initial and intermediate gradient conditions also well as the flow rates listed below were conducted as described in the material and methods section. Drugs listed with a flow rate of 750 to 1500 were run on PE-Sciex API4000. All other drugs were run on PE-Sciex API3000.

Drug	MS Polarity	MRM Transition	Column	Initial Condition	Intermediate Condition	Flow Rate (µl/min)	Internal Standard
Alfentanil	+	417.3 / 268.3	1	95% A : 5% B; 30 sec	10% A : 90%B	750 to 1500	Loperamide
Amprenavir	+	506.4 / 245.4	2	80% A : 20% B	5% A : 95% B	750 to 1500	Ritonavir
Cetirizine	+	389.1 / 201.1	2	95% A : 5% B	5% A : 95% B	750 to 1500	Fexofenadine
Cimetidine	+	253.1 / 159.3	1	95% A : 5% B; 30 sec	10% A : 90%B	750 to 1500	Fexofenadine
Desloratadine	+	311.0 / 259.3	2	95% A : 5% B	5% A : 95% B	750 to 1500	Fexofenadine
Dexamethasone	-	391.2 / 307.3	2	90% A : 5% B : 5% C	5% A : 47.5% B : 47.5% C	500 to 750	Doxorubicin
Digoxin	-	779.5 / 649.5	2	85% A : 15% B	5% A : 95% B	500 to 750	Ivermectin
Diphenhydramine	+	256.1 / 167.3	2	95% A : 5% B	5% A : 95% B	750 to 1500	Fexofenadine
Doxorubicin	-	542.2 / 395.5	2	90% A : 5% B : 5% C	5% A : 47.5% B : 47.5% C	500 to 750	Dexamethasone
Eletriptan	+	383.3 / 84.6	1	95% A : 5% B; 30 sec	10% A : 90%B	750 to 1500	Rizatriptan
Fentanyl	+	337.2 / 188.2	2	80% A : 20% B	5% A : 95% B	750 to 1500	Loperamide
Fexofenadine	+	502.3 / 466.4	2	80% A : 20% B	5% A : 95% B	750 to 1500	Loperamide
Hydroxyzine	+	375.1 / 201.1	2	95% A : 5% B	5% A : 95% B	750 to 1500	Fexofenadine
Indinavir	+	614.5 / 421.5	2	80% A : 20% B	5% A : 95% B	750 to 1500	Ritonavir
Ivermectin	-	873.6 / 229.3	2	85% A : 15% B	5% A : 95% B	500 to 750	Digoxin
Loperamide	+	477.4 / 266.0	2	95% A : 5% B	5% A : 95% B	750 to 1500	Methadone
Loratadine	+	383.0 / 337.1	2	95% A : 5% B	5% A : 95% B	750 to 1500	Fexofenadine
Meperidine	+	248.3 / 220.3	1	95% A : 5% B	5% A : 95% B	750 to 1500	Loperamide
Methadone	+	310.3 / 265.1	2	80% A : 20% B	5% A : 95% B	750 to 1500	loperamide
Morphine	+	286.1 / 201.1	1	95% A : 5% B; 30 sec	20% A : 80% B	750 to 1500	Oxycodone (316.0 / 298.0)
Naratriptan	+	336.1 / 98.4	1	95% A : 5% B; 30 sec	10% A : 90%B	750 to 1500	Zolmitriptan
Nelfinavir	+	568.3 / 330.4	2	80% A : 20% B	5% A : 95% B	750 to 1500	Saquinavir
Paclitaxel	-	852.3 / 525.3	1	95% A : 5% B	5% A : 95% B	750 to 1500	Fexofenadine
Quinidine	+	325.2 / 307.3	2	85% A : 15% B	5% A : 95% B	500 to 750	Olanzapine (325.2 / 307.3)
Ranitidine	+	315.1 / 176.2	1	95% A : 5% B; 30 sec	10% A : 90%B	750 to 1500	Fexofenadine
Ritonavir	+	721.5 / 296.4	2	80% A : 20% B	5% A : 95% B	750 to 1500	Saquinavir
Rizatriptan	+	270.3 / 158.3	1	95% A : 5% B; 30 sec	10% A : 90%B	750 to 1500	Zolmitriptan
Saquinavir	+	671.5 / 570.5	2	80% A : 20% B	5% A : 95% B	750 to 1500	Ritonavir
Sufentanil	+	387.2 / 238.4	1	95% A : 5% B	5% A : 95% B	750 to 1500	Loperamide
Sumatriptan	+	296.1 / 58.5	1	95% A : 5% B; 30 sec	10% A : 90%B	750 to 1500	Zolmitriptan

DMD Fast Forward. Published on January 19, 2007 as DOI: 10.1124/dmd.106.012294
This article has not been copyedited and formatted. The final version may differ from this version.

Triprolidine	+	279.1 / 208.3	2	95% A : 5% B	5% A : 95% B	750 to 1500	Fexofenadine
Verapamil	+	455.4 / 164.9	2	90% A : 5% B : 5% C	5% A : 47.5% B : 47.5% C	500 to 750	Vinblastine
Vinblastine	+	811.6 / 224.1	2	90% A : 5% B : 5% C	5% A : 47.5% B : 47.5% C	500 to 750	Verapamil
Zolmitriptan	+	288.3 / 58.5	1	95% A : 5% B; 30 sec	10% A : 90%B	750 to 1500	Rizatriptan

Table 2. Unbound fractions and $K_{p,brain}$ values for 34 drugs. $K_{p,brain}$ values were determined experimental or obtained from the cited reference. Free fractions are reported as mean ± SD (n=6, unless otherwise indicated by [a] n=4, [b] n=5, [c] n= 16, or [d] n=18).

Drug	$f_{u,plasma}$	$f_{u,brain}$	$K_{p,brain}^{-/-}$	$K_{p,brain}^{+/+}$	Reference for $K_{p,brain}$
Alfentanil (Al)	0.26 ± 0.04	0.32 ± 0.11	0.53	0.19	
Amprenavir (A)	0.075 ± 0.008	0.091 ± .005	1.0	0.072	(Polli et al., 1999)
Cetirizine (C)	0.160 ± 0.009	0.072 ± 0.007	0.080	0.020	(Chen et al., 2003)
Cimetidine (Ci)	0.81 ± 0.07	0.53 ± 0.10	0.031	0.033	
Desloratadine (Dl)	0.055 ± 0.002	0.0071 ± 0.0008	14	<1.0	(Chen et al., 2003)
Dexamethasone (Dex)	0.272 ± 0.014	0.098 ± 0.010[b]	0.70	0.30	(Schinkel et al., 1995b)
Digoxin (Dg)	0.33 ± 0.02	0.0156 ± 0.0011	1.5	0.08	(Schinkel et al., 1995b)
Diphenhydramine (D)	0.33 ± 0.02	0.058 ± 0.003	0.70	9.0	(Chen et al., 2003)
Doxorubicin (Dox)	0.22 ± 0.03	0.0014 ± 0.0005	0.0025	0.00077	(Kusuhara and Sugiyama, 2001)
Eletriptan (Ele)	0.28 ± 0.03	0.055 ± 0.004	14	0.30	(Evans et al., 2003)
Fentanyl (F)	0.17 ± 0.04	0.07 ± 0.005	4.5	2.4	
Fexofenadine (Fex)	0.35 ± 0.03	0.077 ± 0.014	0.30	0.17	(Cvetkovic et al., 1999)
Hydroxyzine (H)	0.062 ± 0.008	0.014 ± 0.002	4.8	3.8	(Chen et al., 2003)
Indinavir (I)	0.058 ± 0.007	0.100 ± 0.008	0.81	0.084	(Kim et al., 1998)
Ivermectin (Iv)	0.024 ± 0.008[b]	0.00009 ± 0.00007[a]	2.5	0.094	(Schinkel et al., 1995a)
Loperamide (Lop)	0.023 ± 0.005[d]	0.0046 ± 0.0005[c]	5.7	0.096	
Loratadine (L)	0.0045 ± 0.00017	0.00178 ± 0.00015	3.3	1.6	(Chen et al., 2003)
Meperidine (Me)	0.38 ± 0.03	0.13 ± 0.019	7.0	6.8	
Methadone (M)	0.147 ± 0.007	0.029 ± 0.002	20	4.0	
Morphine (Mor)	0.50 ± 0.04	0.41 ± 0.11	0.72	0.49	(Schinkel et al., 1995b)
Naratriptan (N)	0.58 ± 0.03	0.23 ± 0.02	1.1	0.42	(Evans et al., 2003)
Nelfinavir (Nel)	0.0010 ± 0.0004	0.00053 ± 0.00004	2.6	0.086	(Kim et al., 1998)
Paclitaxel (Pax)	0.021 ± 0.002	0.0028 ± 0.0004	4.0	0.50	(Kemper et al., 2004)
Quinidine (Q)	0.16 ± 0.03	0.037 ± 0.003	4.8	0.20	(Kusuhara et al., 1997)
Ranitidine (Ra)	0.96 ± 0.05	0.96 ± 0.13	0.039	0.022	
Ritonavir (Rit)	0.0027 ± 0.0005	0.0106 ± 0.0016	2.3	0.17	(Yamazaki et al., 2001)
Rizatriptan (Riz)	0.62 ± 0.02	0.348 ± 0.014	0.85	0.20	(Evans et al., 2003)
Saquinavir (Sq)	0.00043 ± 0.00007	0.00190 ± 0.00016	0.88	0.13	(Kim et al., 1998)
Sufentanil (Su)	0.054 ± 0.014	0.034 ± 0.010	4.8	1.6	
Sumatriptan (Sum)	0.63 ± 0.03	0.36 ± 0.03	0.22	0.13	(Evans et al., 2003)
Triprolidine (T)	0.31 ± 0.02	0.092 ± 0.002	3.6	5.9	(Chen et al., 2003)
Verapamil (V)	0.11 ± 0.03	0.033 ± 0.02	3.3	0.43	(Hendrikse et al., 1998)
Vinblastine (Vi)	≥ 0.09	0.0046 ± 0.0004	19	1.7	(Schinkel et al., 1994)
Zolmitriptan (Z)	0.98 ± 0.11[b]	0.54 ± 0.08	0.085	0.038	(Evans et al., 2003)

DMD Fast Forward. Published on January 19, 2007 as DOI: 10.1124/dmd.106.012294
This article has not been copyedited and formatted. The final version may differ from this version.

Table 3. Classification of drugs based on discrepancies between in vivo P-gp efflux ratio and $[plasma]_{,u}/[brain]_{,u}$ ratio. The classification for each drug was assigned according to the scheme in Figure 1. Additional evidence from the literature is provided to support of classification of each drug.

Class Ib P-gp efflux + additional mechanism		Class II Weak or no P-gp efflux + additional impairment		Class IV P-gp efflux – compensatory mechanism(s)	
Drug	Additional Evidence	Drug	Additional Evidence	Drug	Additional Evidence
Cetirizine (C)	very low permeability (Mahar Doan et al., 2002)	Cimetidine (Ci)	Non-Pgp efflux transporter(s) (www.tp-search.jp)	Methadone (M)	active uptake (Chi and Dixit, 1977)
Digoxin (Dg)	additional efflux transporter(s) (www.tp-search.jp)	Dexamethasone (Dex)	steroid transporter (Pariante et al., 2001)	Ritonavir (Rit)	active uptake (Anthonypillai et al., 2004)
Doxorubicin (Dox)	additional efflux transporter(s) (www.tp-search.jp)	Fexofenadine (Fex)	reduced CNS activity (Hindmarch et al., 2002)	Saquinavir (Sq)	active uptake (Su et al., 2004)
Ivermectin (Iv)	additional efflux transporter(s) (Lespine et al., 2005)	Ranitidine (Ra)	Non-Pgp efflux transporter(s) (Bourdet et al., 2005)		
		Sumatriptan (Sum)	very low permeability (Mahar Doan et al., 2002)		
		Zolmitriptan (Z)	very low permeability (Mahar Doan et al., 2002)		

DMD Fast Forward. Published on January 19, 2007 as DOI: 10.1124/dmd.106.012294
This article has not been copyedited and formatted. The final version may differ from this version.

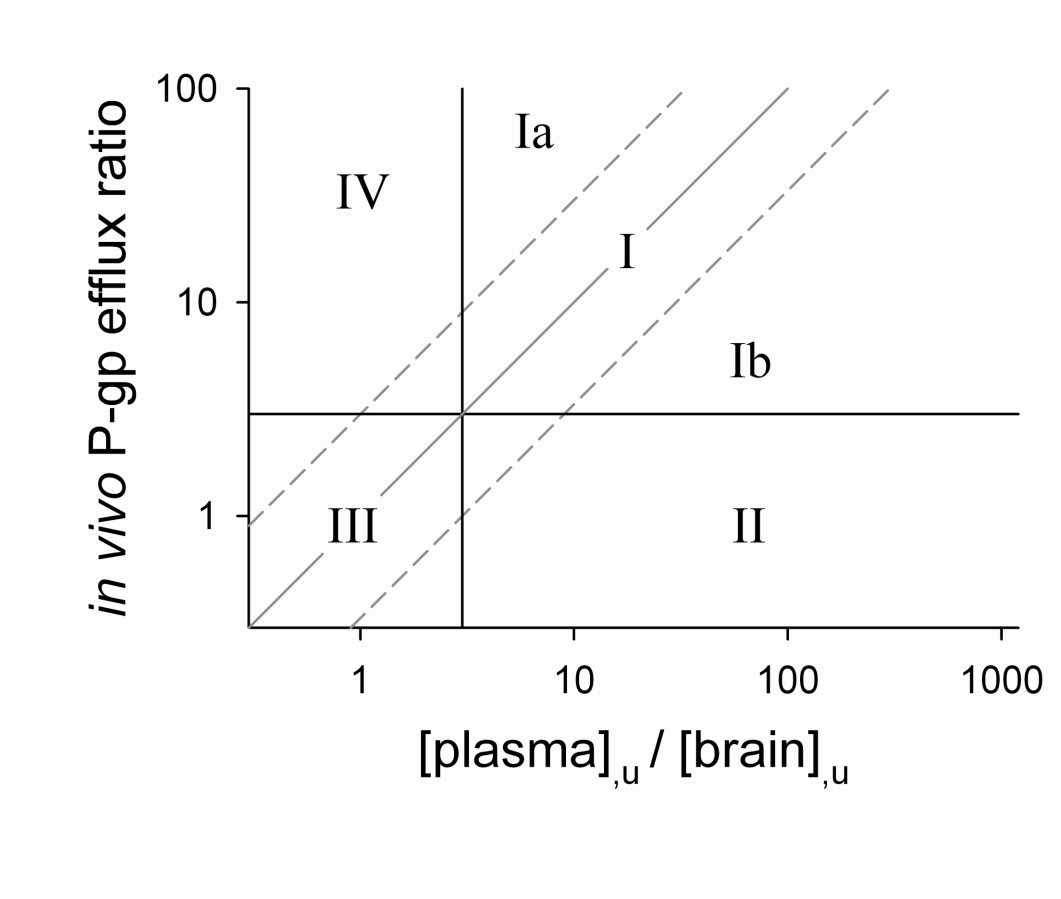

Figure 1

DMD Fast Forward. Published on January 19, 2007 as DOI: 10.1124/dmd.106.012294
This article has not been copyedited and formatted. The final version may differ from this version.

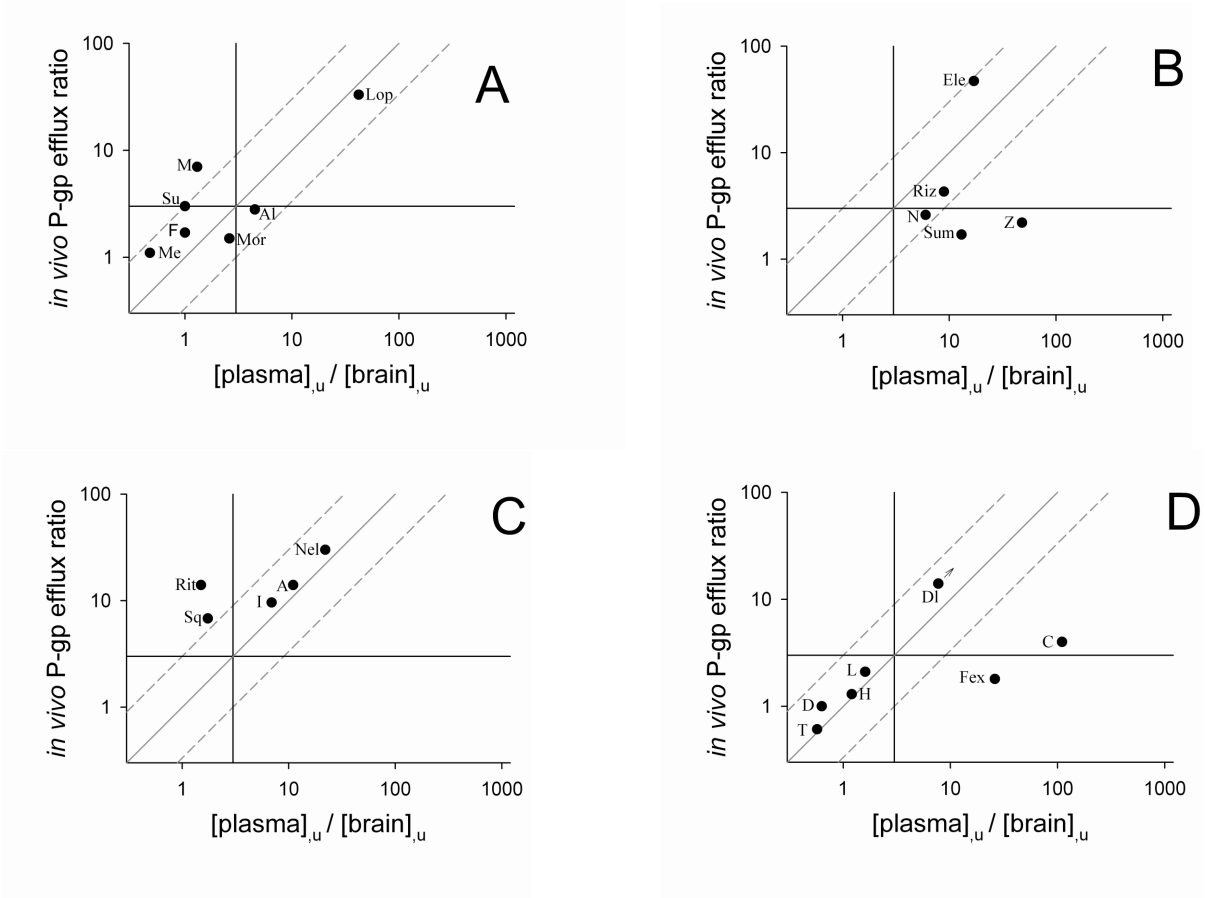

Figure 2

DMD Fast Forward. Published on January 19, 2007 as DOI: 10.1124/dmd.106.012294
This article has not been copyedited and formatted. The final version may differ from this version.

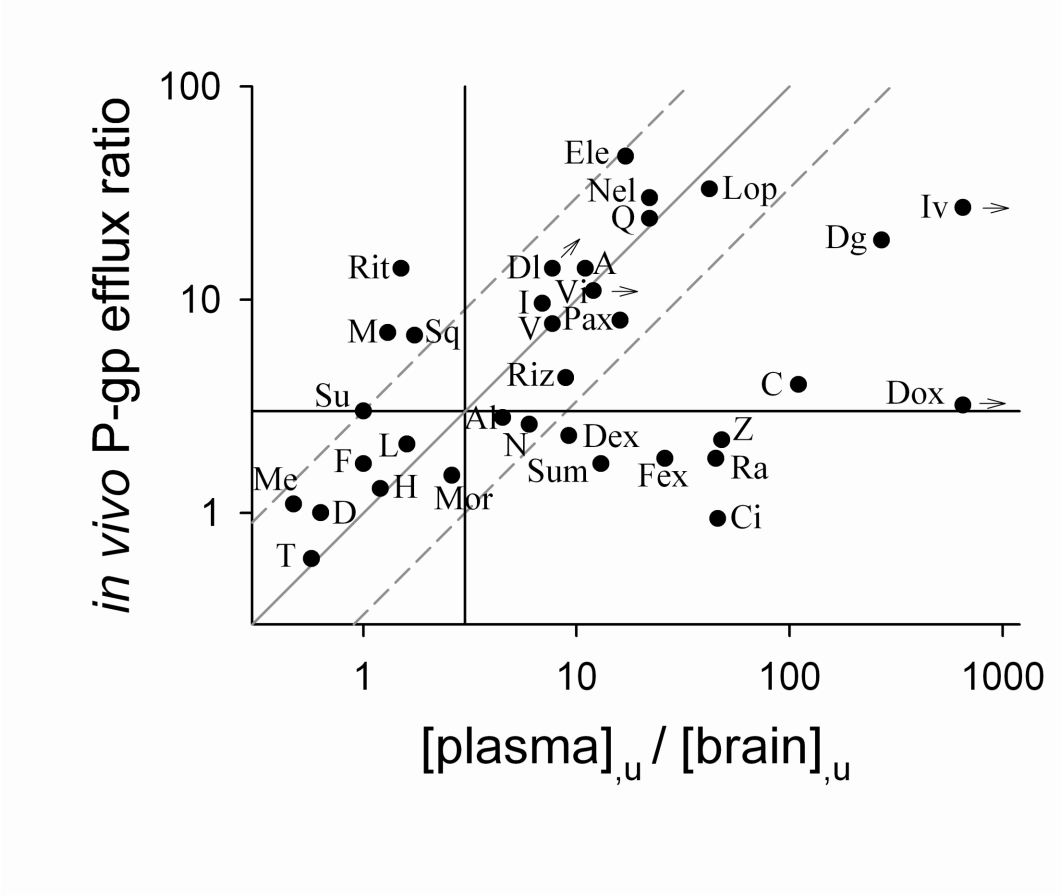

Figure 3